EPJ Web of Conferences **345**, 01077 (2026) https://doi.org/10.1051/epjconf/202634501077
ICE3MT2025

Preparation and characterization of activated charcoal from a plant mixture and its use in the adsorption of methyl orange dye from aqueous solutions, a chemical and thermodynamic study

Jwan Abdulwahid Oleiwi [*], *Liqaa Hussein* Alwan, and *Diana AbdAlkreem* Al-Rifaie

Department of Applied Chemistry, Samarra University, Samarra, Iraq

Abstract. Water pollution from industrial effluents, particularly those containing synthetic dyes, poses a serious environmental and health threat due to their toxicity, persistence, and resistance to conventional treatment methods. Developing sustainable and cost-effective adsorbents is therefore of great importance. In this work, nano-activated carbon was synthesized from a mixture of wormwood and acacia seed pods and evaluated for the removal of orange dye from aqueous solutions. The adsorbent showed high efficiency, achieving 95% removal within 40 minutes. The effects of contact time, temperature, and adsorbent dosage were systematically investigated. Kinetic analysis indicated that the adsorption process followed the pseudo-second-order model, while thermodynamic results confirmed that the process was endothermic and spontaneous at all studied temperatures, as shown by negative Gibbs free energy values. Positive entropy changes suggested increased randomness at the solid–solution interface, and equilibrium data fitted well to the Freundlich model, indicating heterogeneous multilayer adsorption. Overall, the findings demonstrate that the adsorption mechanism is mainly physical in nature and highlight the potential of this green-synthesized nano-activated carbon as an efficient and eco-friendly material for treating dye-contaminated wastewater.

1 Introduction

The increasing demand for dyes in the expanding industrial sector has resulted in the generation of large volumes of dye-containing wastewater, particularly from textile industries. The discharge of colored effluents into surface water bodies severely impacts aquatic ecosystems, human health, and animal life, thereby posing a global environmental concern [1]. For decades, millions of people worldwide have suffered from multi-drug-resistant infections and carcinogenic diseases caused by contaminated water containing harmful dyes and microbes. The shortage of cost-effective and safe drinking water compels societies to develop new materials and strategies to mitigate these challenges [2] Among synthetic dyes, anionic azo dyes represent a significant fraction of wastewater due to their

[*] Corresponding author: jwan.a@uosamarra.edu.iq

poor binding to natural fibers [3]. *Methyl orange (MO)*, a water-soluble azo dye, is widely used because

of its strong coloring ability and bright orange color. However, MO and other azo dyes contain aromatic and –N=N– groups that are toxic, carcinogenic, and teratogenic, making them highly harmful to both the environment and living organisms [4]. Therefore, effective treatment methods for their safe removal are urgently required. Adsorption has been recognized as one of the most efficient techniques for eliminating such pollutants from aqueous media [5] Parallel to these advancements, biochar and activated carbons derived from plant residues have gained importance as low-cost, sustainable, and efficient adsorbents for wastewater treatment [6]. Biochar shows notable advantages including broad feedstock availability, simple preparation methods, and favorable surface and structural characteristics. Activated charcoal prepared from natural plants such as *Acacia* has been successfully applied for dye adsorption as a cheap and eco-friendly alternative [7]. Similarly, charcoal derived from *Artemisia vulgaris* (wormwood), a pharmaceutical by-product, has demonstrated high efficiency and good reusability in the adsorption of pollutants such as orange peel dye [8, 9]. Depending on these findings, the present investigation explores the potential of activated carbon prepared from a mixture of wormwood (*Artemisia vulgaris*) and acacia plants. By combining these two plant sources in specific proportions, a novel adsorbent with enhanced adsorption efficiency toward methyl orange dye is proposed. This strategy aims to integrate the advantages of bio-based activated carbons with nanoscale adsorption mechanisms for sustainable water purification

2 Experimental section

2.1 Materials

Wormwood leaves, acacia seed pods, methyl orange dyeMO, hydrochloric acid HCl, and sodium hydroxide NaOH .

2.2 Activated charcoal preparation

Both wormwood leaves and acacia seed pods were thoroughly washed with distilled water and dried in a drying oven at 100°C for 3 hours. The two herbs were then ground separately, and specific proportions of each plant were taken to prepare five charcoal samples at different ratios and determine the efficiency of each. Sample No. 4 was found to be the best among all the samples, yielding the highest adsorption efficiency. The specified proportions of each sample were placed in a ceramic bowl in a kiln at 650°C for an hour to activate the formation of activated carbon. The charcoal was then activated with 1 M hydrochloric acid and returned to the kiln for another hour. The acidity of all samples was measured and found to be close to pH 7. Table (1) shows the results of the efficiency of the prepared charcoal [10].

Table 1. The charcoal samples prepared from wormwood leaves and acacia seed pods and the efficiency of each sample in adsorption of methyl orange dye.

Ci(ppm)	Model C1 100% wormwood leave plant	Model C2 50% wormwood leave 50% Acacia seed pods	Model C3 100% Acacia Seed Pods	Model C 4 75% wormwood leaves 25% acacia seed pods	Model C5 25% wormwood leaves 75% acacia seed pods	T (min)	activated charcoal weight (gm)
24	A 0.223	0.243	0.325	0.134	0.412	40	0.05
24	Ce 2.478	2.747	3.853	1.278	5.025	40	0.05
24	Ads% 89.6%	88.5%	83.9%	94%	79%	40	0.05

2.3 Instrumentation

The instrumentations used in this study were UVvis spectrophotometers (Perkin Elmer, Lambda 35), Xray diffraction spectroscopy (S-4800, Hitachi, Japan), FTIR spectroscopy (8400S, Shimadzu, Japan). Field emission scanning electron microscope (FE-SEM, MIRA3, TESCAN, Iran) with an accelerating voltage of 15 kV.

3 Results and discussion

3.1 FT-IR spectrum interpretation

The infrared spectrum of the banned activated charcoal was measured to determine whether the charcoal contained active groups. The spectrum in Figure 1 shows that the banned activated charcoal does not contain an active group that might affect the adsorption process of the dye used in this study. This is a good characteristic of the banned charcoal. The Figure 1 represents a spectrum of activated charcoal.

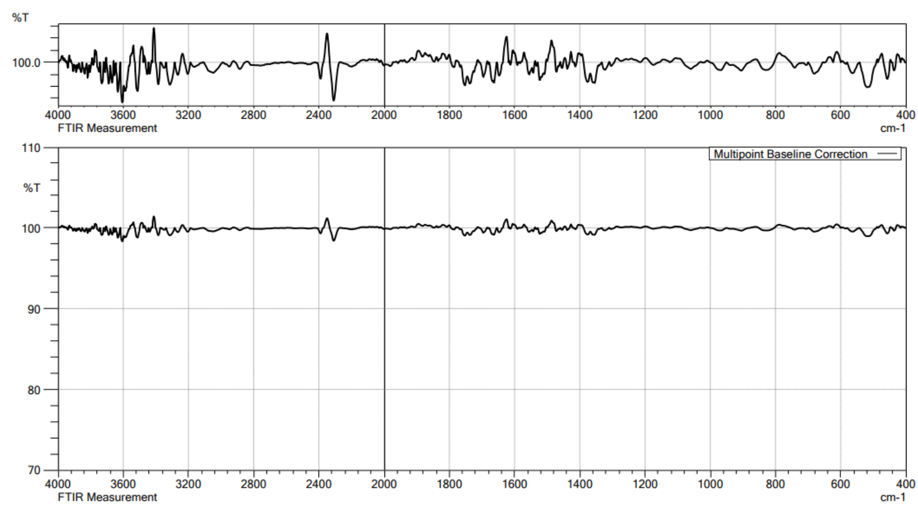

Fig. 1. Spectrum of activated charcoal.

3.2 EDX

The spectrum of nano-activated carbon showed main peaks at energies corresponding to carbon, which confirms the dominant carbon nature of the structure, in addition to a clear peak for oxygen, indicating the presence of oxygen functional groups on the surface, as well as peaks for minor mineral elements such as (sulfur, potassium, magnesium, and calcium), which may be derived from ash residues or components of the raw material. These results confirm the carbon structure, making activated carbon a promising material for treating pollutants in water. Table (2) shows the percentages of elements in activated charcoal. Figure 2 shows the proportions of elements in the blocked absorbing surface activated charcoal.

Table 2. EDX analysis shows the element values in activated charcoal.

Elt	Line	Int	Error	K	Kr	W%	A%	Ox%	Pk/Bg	Class	LConf	HConf
C	Ka	491.1	42.3196	0.2442	0.0978	56.92	75.33	0.00	871.84	A	56.25	57.58
O	Ka	58.6	42.3196	0.0296	0.0119	8.03	7.97	0.00	94.74	A	7.75	8.30
Mg	Ka	67.8	56.8997	0.0359	0.0144	2.04	1.33	0.00	24.77	A	1.98	2.10
Al	Ka	65.0	56.8997	0.0349	0.0140	1.83	1.08	0.00	19.41	A	1.77	1.89
Si	Ka	161.9	56.8997	0.0883	0.0353	4.22	2.39	0.00	40.42	A	4.14	4.31
P	Ka	67.2	56.8997	0.0372	0.0149	1.80	0.92	0.00	15.43	A	1.74	1.86
S	Ka	86.1	56.8997	0.0486	0.0194	2.22	1.10	0.00	19.71	A	2.16	2.28
Cl	Ka	518.7	56.8997	0.2979	0.1192	14.21	6.37	0.00	109.83	A	14.05	14.38
K	Ka	98.0	23.3204	0.0585	0.0234	2.82	1.15	0.00	18.84	A	2.75	2.90
Ca	Ka	205.0	23.3204	0.1249	0.0500	5.91	2.34	0.00	35.04	A	5.80	6.01
				1.0000	0.4003	100.00	100.00	0.00				

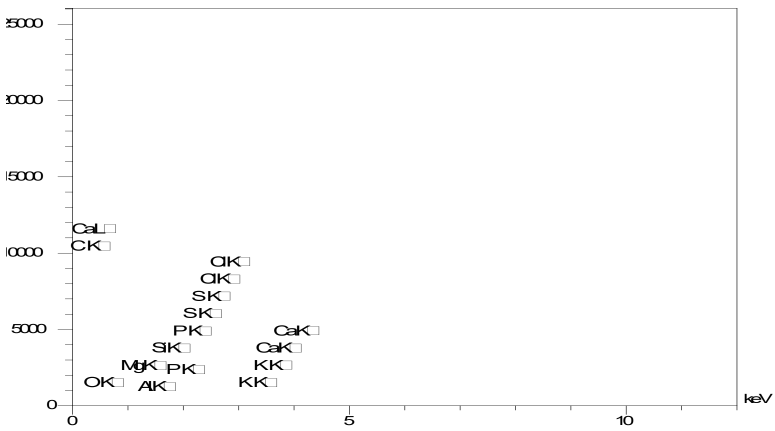

Fig. 2. Represent the proportions of elements in the blocked absorbing surface activated charcoal.

3.3 XRD technology

The X-ray diffraction (XRD) pattern of the activated carbon shown in Figure 3 shows a broad halo between 20–30° (2θ), corresponding to the (002) reflection of turbostratic carbon. This indicates a disordered arrangement of graphene-like layers with an interlayer spacing larger than that of crystalline graphite, confirming the amorphous and porous nature of the material. Several sharp peaks at 20.8°, 26.6°, 28.3°, 39.4°, 40.5°, 42.4°, 45.4°, 50.2°, 60.0°, 66.4°, 68.2°, and 73.7° are attributed to α-quartz, reflecting siliceous ash derived from the plant precursor. The broadening of the (002) reflection suggests a crystallite size of only a few nanometers, emphasizing the nanoscale domains and structural disorder that enhance the adsorption efficiency of the activated carbon.

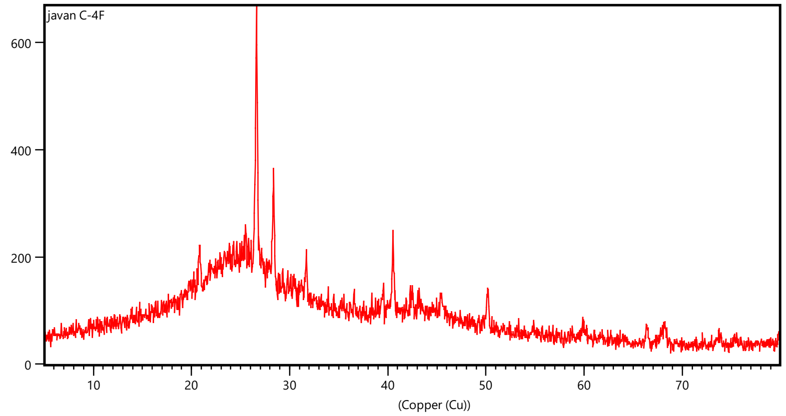

Fig. 3. Represents the X-ray diffraction measurement of the studied nanocomposite. activated charcoal.

3.4 SEM technology

Scanning electron microscope (SEM) images illustrated in Figure 4, of activated charcoal prepared from the herbal mixture revealed a heterogeneous surface structure composed of nanoparticles ranging in diameter from 25 to 66 nm, with larger aggregates is observed. The images also revealed the presence of spherical particles bound to the surface of the material, along with fractured sheets and microcracks, reflecting a multi-level porous structure (micro–meso–macro pores). This irregular particle distribution and the morphological diversity between nanospheres and lamellar layers enhance the specific surface area and provide a large number of effective sites for pollutant adsorption. Furthermore, the porous appearance and cracks resulting from the activation process facilitate the diffusion of colored organic molecules within the carbon structure, making the prepared activated charcoal a promising material for treating industrial wastewater contaminated with dyes.

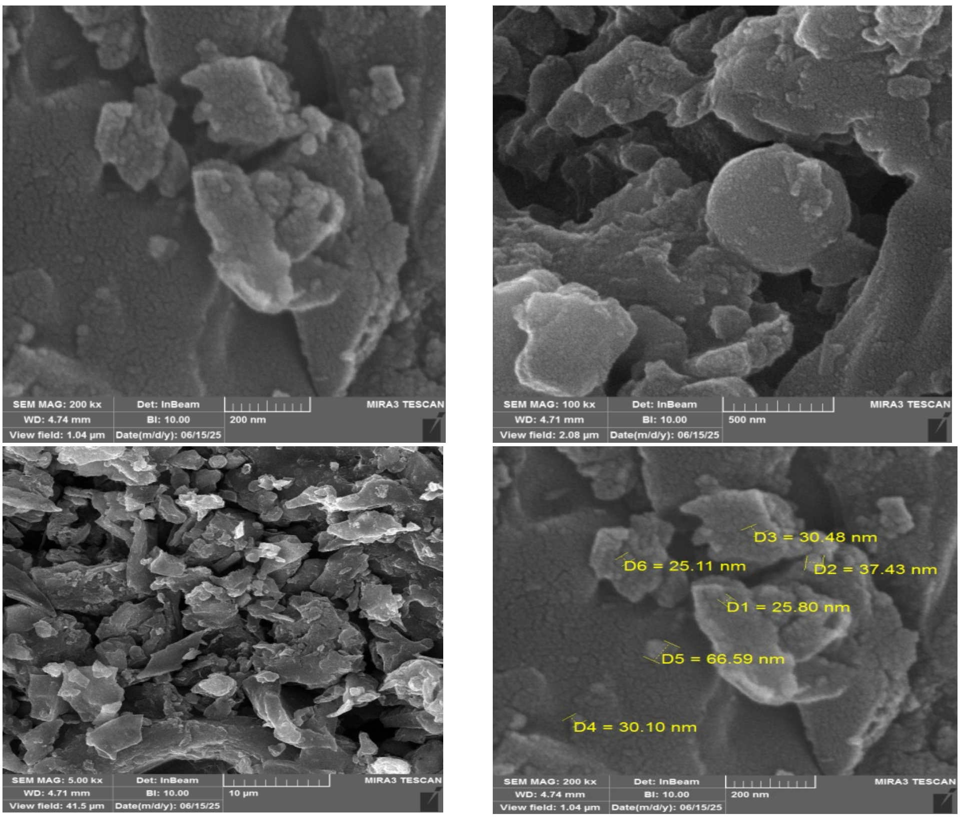

Fig. 4. Scanning electron microscope images SEM.

3.5 Adsorption kinetics study

Nanomaterial-based adsorption, such asactivated charcoal , carbon nanotubes (CNT), metals, metal oxides, and graphene, offers significant advantages due to their large surface area, superior reactivity, and rapid kinetics, making them highly feasible for wastewater treatment in the industrial sector [11]. To ensure effectiveness, an adsorption material must demonstrate high adsorption capacity, inertness, biocompatibility, and resistance to mechanical forces. The main driving forces behind adsorption are electrostatic interactions and Van der Waals forces,

The adsorption capacity of a given material varies depending on the system in which it is applied, as the rate of adsorption changes with the exposure time of the adsorbent to the pollutant ,Studying the adsorption kinetics is crucial for evaluating the adsorption efficiency, determining the rate of adsorption, and assessing the effectiveness of the adsorbent. Several models have been proposed to describe the adsorption kinetics In this study, the experimental kinetic results were evaluated using different kinetic models. Among these, the applicability of pseudo-first-order and pseudo-second-order kinetic models was selected. The pseudo-first-order equation (1) and the pseudo-second-order equation (2) can be expressed as follows: [12].

The pseudo-first-order equation (1)

$$\frac{t}{qt} = \frac{1}{k2qe2} + \frac{1}{qe} \text{........ equation (1)}$$

Where:

t: contact time.
qt: amount of adsorbate adsorbed at time t.
qe: amount of adsorbate adsorbed at equilibrium.
k2: pseudo–second-order rate constant

Figure 5 shows the graph between pseudo-first-order kinetics of methyl Orang dye with the adsorbent surface at different temperatures.

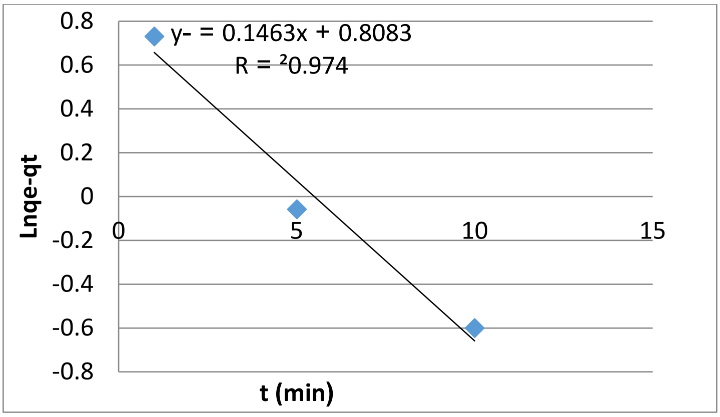

Fig. 5. The pseudo-first-order kinetics of methyl Orang dye with the adsorbent surface at different temperatures.

The pseudo-second-order equation (2)

$$\frac{Ce}{Qe} = \frac{1}{QmaxKL} + \frac{Ce}{Qmax} \text{........ equation (2)}$$

Where:
Ce: equilibrium concentration.
Qe : amount of adsorbate adsorbed at equilibrium.
Qmax: maximum monolayer adsorption capacity.
KL: Langmuir constant.

Figure 6 shows the application of the data to the second-order equation.

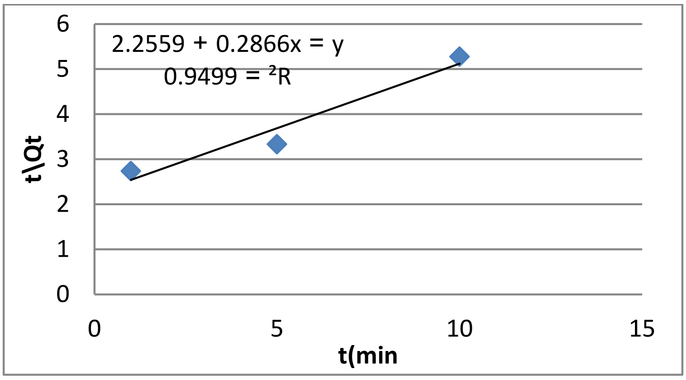

Fig. 6. Represents the application of the data to the second-order equation.

3.6 Adsorption isotherms

Adsorption is a versatile and effective method for removing pollutants from industrial water of various types, whether dyes or heavy metals, which includes the use of low-cost and highly efficient absorbent materials. It has been developed significantly in recent years. To understand this phenomenon, the Langmuir and Freundlich models were applied to the study data to determine which one matches the results obtained.
The Langmuir adsorption equation was used, which is based on the fact that the maximum adsorption corresponds to a saturated monolayer of dissolved material molecules on the surface of the absorbent material. The equation is represented in linear form in Equation(3) [13]

$$\frac{Ce}{Qe} = \frac{1}{QmaxKL} + \frac{Ce}{Qmax} \quad \text{........ equation (3)}$$

Where:

Ce: equilibrium concentration.
Qe : amount of adsorbate adsorbed at equilibrium.
Qmax: maximum monolayer adsorption capacity.
KL: Langmuir constant.

Table 3. Adsorption data of methyl Orang on activated charcoal at different temperatures by adsorption data of the Langmuir isotherm model.

The Absorbent Surface	Temperature (K)	K_L	Qmax	R^2
activated charcoal	288	0.111	9.354	05906
	298	0.173	8.361	0.6597
	308	0.476	8.103	0.7393
	318	0.473	8.169	0.871

We note from Table (3) that the value of the correlation coefficient R^2 has low values, which indicates less suitability for the Langmuir model and suggests that the adsorption of methyl orange on the surface of the prepared activated carbon does not accurately follow the monolayer adsorption model on homogeneous surfaces

The Freundlich equation was also applied, which is an equation that describes adsorption on heterogeneous solid surfaces. This type is used to describe multi-layer adsorption, not just single-layer adsorption, and depends on heterogeneous systems in adsorption. The Freundlich equation is represented in linear form as Equation 4

$$\ln Qe = \ln Kf + \frac{1}{n}\ln Ce \quad \text{………. Equation (4)}$$

where:
Qe: amount of adsorbate adsorbed at equilibrium.
Ce: equilibrium concentration.
Kf: Freundlich adsorption constant
1/n: heterogeneity factor.

Table 4. Adsorption data of methyl Orang on activated charcoal at different temperatures by the Freundlich isotherm model.

The Absorbent Surface	Temperature (K)	K_F	n	R^2
activated charcoal	288(k)	1.405	1.859	0.8407
	298(K)	1.835	2.194	0.8004
	308(K)	2.545	2.812	0.7953
	308(K)	3.296	3.214	0.8843

We note from the values in Table (4) for the Freundlich model that the value of the correlation coefficient R^2 is high, which indicates the suitability of this model and that the adsorption of methyl orange on the surface of the prepared activated carbon accurately follows the multi-layer model on heterogeneous surfaces [14].

3.7 Thermodynamic constants

The thermodynamic functions, including Kipps free energy, enthalpy, and entropy change, were calculated. After applying them to the data obtained from the experiment, the results were presented in Table (5).

Table 5. Represents the values of the thermodynamic functions for methyl orange adsorption.

T(K)	Δ G(J.mol-1)	ΔH (J.mol-1)	ΔS (J.mol-1 k-1)
288	-2102.311	41608.244	151.772
298	-3017.682	41608.244	149.751
308	-4916.567	41608.244	151.054
318	-6580.547	41608.244	151.537

It was found that the enthalpy of adsorption of the orange dye onto the prepared charcoal was positive, indicating that the adsorption process is endothermic.
The Kipps free energy value was negative for all temperatures, indicating that the reaction occurred spontaneously.

The entropy change for the adsorption of the orange dye onto the prepared charcoal surface was positive, indicating that the adsorbed dye molecules are irregular (increased randomness) on the surface when adsorption and desorption occur together. That is, the more the concentration of molecules on the surface increases, the more randomness occurs
Observing the enthalpy value shows that the adsorption is of the physical adsorption type.

3.8 The effect of factors on the adsorption process

1- The effect of contact time

The effect of time is one of the most important variables that can be used to evaluate experimental data for the adsorption process, especially the kinetic study. All variables related to the adsorption process were fixed, except for time, at an initial concentration of 24 ppm of methyl orange dye in a volume of 20 ml and a fixed amount of adsorbent (0.05) grams of activated carbon at a temperature of 25°C. The results are presented in Table (6).

Table 6. Effect of contact time on adsorption capacity at 25°C and an initial concentration of (8) ppm.

The Absorbent Surface	Adsorbent	Time(min)	Ci(ppm)	Ct	qt
activated charcoal	MO	1	8	7.087	0.365
	MO	5	8	4.252	1.499
	MO	10	8	2.265	1.894
	MO	20	8	2.136	2.345
	MO	30	8	1.826	2.469
	MO	40	8	1.713	2.514

The results shown in the previous table indicate that the efficiency of activated carbon to adsorb the orange dye ranged between 91% and 94% over a period of (40) minutes, which is the equilibrium time. The percentage of the adsorbed material increases with time, and the adsorption process remains almost constant at equilibrium.

3.9 Effect of temperature

Temperature directly affects the adsorption process. Through this, some properties of the process can be determined, whether it is exothermic or endothermic. This process also affects the efficiency of the adsorption process [15]. In this study, the adsorption efficiency was calculated at different temperatures (288,298,308,318) and a fixed initial concentration (24) ppm. The experimental data were presented in a table (7). It was observed that the adsorption efficiency of the orange dye on the activated carbon surface increases as the temperature increases. This is due to surface expansion, which increases the surface area. This leads to an increase in the number of active sites, in addition to the possibility of providing the kinetic energy necessary for the adsorption process to occur. This causes the dye molecules to enter the adsorbent surface structure, thus increasing the amount of adsorbed dye. Figure 7 shows the relationship between the residual concentration and the adsorption capacity at different temperatures.

Table 7. Represents the values of the effect of temperature for methyl Orang adsorption.

T(K)	Qe	$Ads\%$
288	9.0564	94.3%
298	9.0888	94.6%
308	9.1328	95%
318	9.1372	95.1%

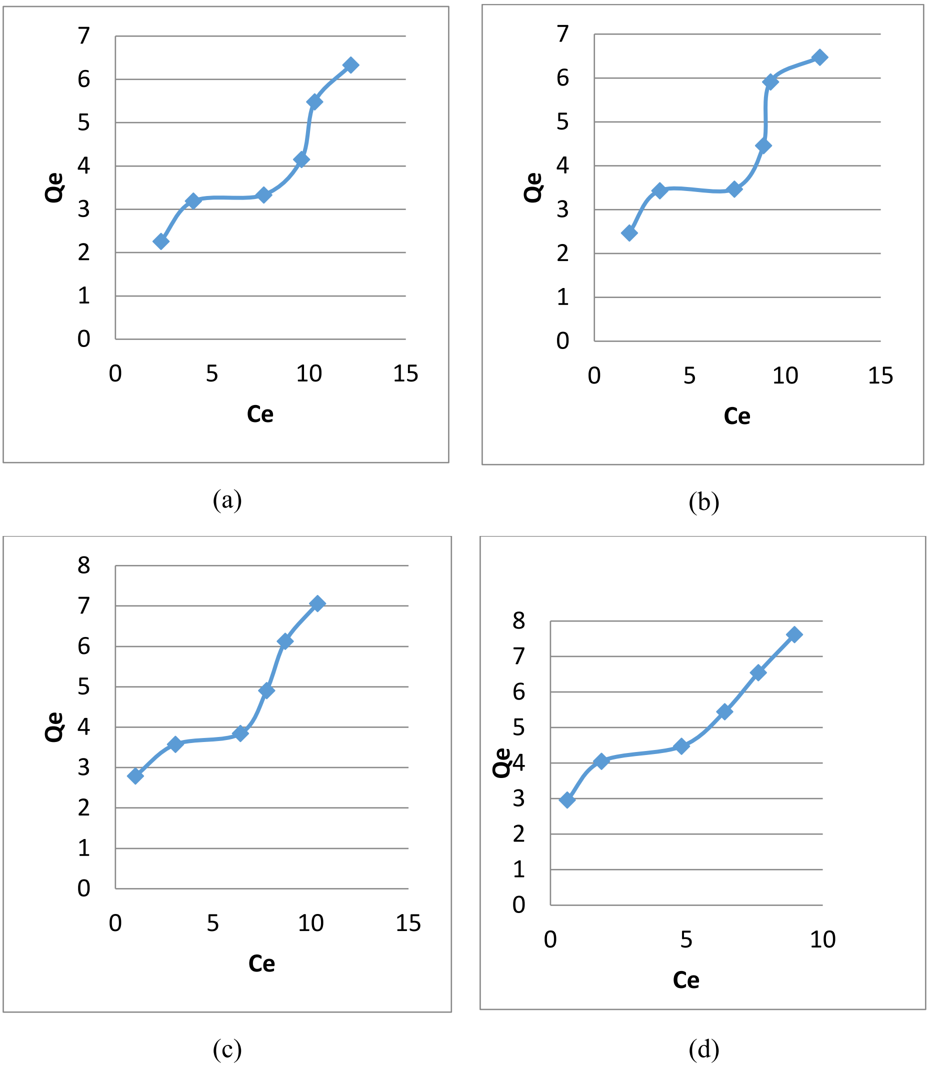

Fig. 7. Represents the relationship between the residual concentration and the adsorption capacity at different temperatures : (a) 288 K, (b) 298 K, (c) 308 K, and (d) 318 K.

3.9 Effect of adsorbent dose

Several doses were taken to weigh the adsorbent (activated carbon) and determine its effect on the adsorption efficiency and adsorption capacity. It was noted that the weight of the adsorbent surface that gives the highest adsorption efficiency is (0.05) grams. The results are shown in Table (8).

Table 8. Effect of concentration on adsorption capacity at 25°C.

Adsorbent	Dose (gm)	Ci (ppm)	Qe	Ads%
MO	0.01	8	1.634	51%
MO	0.03	8	1.894	59%
MO	0.05	8	2.514	78%

4 Conclusion

This research aims to prepare environmentally friendly adsorbent materials from safe and inexpensive materials. Nano-activated carbon was prepared from wormwood plant and acacia seed pods and proved its effectiveness in adsorbing the toxic orange dye from its aqueous solutions with a high efficiency of up to 95%. The prepared activated charcoal demonstrated high adsorption efficiency driven by its multi-scale porous structure, fast kinetics, and strong affinity for methyl orange dye. Overall, the kinetic, isotherm, and thermodynamic analyses confirm that adsorption proceeds spontaneously through endothermic physical interactions, making the material a highly promising adsorbent for wastewater treatment applications.

References

1. Khan, M. D., Singh, A., Khan, M. Z., Tabraiz, S., & Sheikh, J. (2023). Current perspectives, recent advancements, and efficiencies of various dye-containing wastewater treatment technologies. Journal of Water Process Engineering, 53, 103579.)
2. Sun, H., Jiang, J., Xiao, Y., & Du, J. (2018). Efficient removal of polycyclic aromatic hydrocarbons, dyes, and heavy metal ions by a homopolymer vesicle. ACS applied materials & interfaces, 10(1), 713-722.).
3. Bai, Y. N., Wang, X. N., Zhang, F., Wu, J., Zhang, W., Lu, Y. Z., ... & Zeng, R. J. (2020). High-rate anaerobic decolorization of methyl orange from synthetic azo dye wastewater in a methane-based hollow fiber membrane bioreactor. Journal of hazardous materials, 388, 121753.
4. Haque, M. M., Haque, M. A., Mosharaf, M. K., & Marcus, P. K. (2021). Decolorization, degradation and detoxification of carcinogenic sulfonated azo dye methyl orange by newly developed biofilm consortia. Saudi Journal of Biological Sciences, 28(1), 793-804.
5. Wu, L., Liu, X., Lv, G., Zhu, R., Tian, L., Liu, M., ... & Liao, L. (2021). Study on the adsorption properties of methyl orange by natural one-dimensional nano-mineral materials with different structures. Scientific reports, 11(1), 10640.
6. Heo, J. W., An, L., Chen, J., Bae, J. H., & Kim, Y. S. (2022). Preparation of amine-functionalized lignins for the selective adsorption of Methylene blue and Congo red. Chemosphere, 295, 133815.
7. Saleem, M., Ali, M., Siddiqi, Z., & Al Qahtani, A. S. (2017). Preparation of activated carbon from acacia (Vachellia seyal) Tree Branches and application to treat wastewater containing methylene blue dye. Modern Applied Science, 11(12), 102.
8. Kenza, A., Bensmaili, A., Bouafia-Chergui, S., & Kadmi, Y. (2020). New activated carbon from wormwood as efficient adsorbent of cationic dye in aqueous solution. *Iranian Journal of Chemistry and Chemical Engineering (IJCCE)*, *39*(6), 137-148.)
9. Wang, S., Huang, Y., Wu, Y., Zhang, X., Wan, L., Liu, X., & Zhang, W. (2021). Re-utilization of Chinese medicinal herbal residue: waste wormwood rod-derived porous carbon as a low-cost adsorbent for methyl orange removal. *Water Science and Technology*, *84*(9), 2601-2614).
10. Kiran, M., Haq, F., Mehmood, S., & Aziz, T. (2025). Innovative biosorbents from agro-waste: Advancing sustainable solutions for heavy metal, dye, and organic pollutant removal. J Chem Eng Res Updates, 12, 1-33.

11. Ahmed, S. F., Kumar, P. S., Rozbu, M. R., Chowdhury, A. T., Nuzhat, S., Rafa, N., ... & Mofijur, M. (2022). Heavy metal toxicity, sources, and remediation techniques for contaminated water and soil. Environmental Technology & Innovation, 25, 102114.
12. Zhao, B., Xiao, W., Shang, Y., Zhu, H., & Han, R. (2017). Adsorption of light green anionic dye using cationic surfactant-modified peanut husk in batch mode. Arabian Journal of Chemistry, 10, S3595-S3602.
13. Arıca, M. Y., Bayramoğlu, G., Yılmaz, M., Bektaş, S., & Genç, Ö. (2004). Biosorption of Hg2+, Cd2+, and Zn2+ by Ca-alginate and immobilized wood-rotting fungus Funalia trogii. Journal of Hazardous Materials, 109(1-3), 191-199.
14. Bülbül, A., Delibaş, A., & Coşkun, R. (2025). Development and characterization of activated charcoal adsorbent derived from oak for efficient removal of methylene blue: functionality vs surface area. Biomass Conversion and Biorefinery, 1-16.
15. Laccourreye, O., & Maisonneuve, H. (2019). French scientific medical journals confronted by developments in medical writing and the transformation of the medical press. European Annals of Otorhinolaryngology, Head and Neck Diseases, 136(6), 475-480.